Original Article

Non-invasive estimation of vascular compliance and distensibility in the arm vessels: a novel ultrasound-based protocol

Sara Cappelletti[1,2], Alessandro Caimi[1]^, Alice Caldiroli[3], Irene Baroni[4]^, Emiliano Votta[1,5]^, Stefania A. Riboldi[2]^, Massimiliano M. Marrocco-Trischitta[4,6]^, Alberto Redaelli[1]^, Francesco Sturla[1,5]^*

[1]Department of Electronics, Information and Bioengineering, Politecnico di Milano, Milan, Italy; [2]Dialybrid Srl, Cantù, Italy; [3]Bioengineering Laboratories Srl, Cantù, Italy; [4]Clinical Research Unit, Cardiovascular Department, IRCCS Policlinico San Donato, San Donato Milanese, Italy; [5]3D and Computer Simulation Laboratory, IRCCS Policlinico San Donato, San Donato Milanese, Italy; [6]Vascular Surgery Unit, Cardiovascular Department, IRCCS Policlinico San Donato, San Donato Milanese, Italy

Contributions: (I) Conception and design: S Cappelletti, F Sturla, A Redaelli; (II) Administrative support: E Votta, MM Marrocco-Trischitta, F Sturla, A Redaelli; (III) Provision of study materials or patients: SA Riboldi, MM Marrocco-Trischitta, I Baroni; (IV) Collection and assembly of data: S Cappelletti, A Caimi, A Caldiroli, F Sturla; (V) Data analysis and interpretation: S Cappelletti, A Caimi, F Sturla; (VI) Manuscript writing: All authors; (VII) Final approval of manuscript: All authors.

Correspondence to: Francesco Sturla, PhD. 3D and Computer Simulation Laboratory, IRCCS Policlinico San Donato, Piazza Edmondo Malan 2, San Donato Milanese 20097, Italy. Email: francesco.sturla@grupposandonato.it.

Background: Performance and durability of arterio-venous grafts depend on their ability to mimic the mechanical behavior of the anastomized blood vessels. To select the most suitable synthetic graft, *in vivo* evaluation of the radial deformability of peripheral arteries and veins could be crucial; however, a standardized non-invasive strategy is still missing. Herein, we sought to define a novel and user-friendly clinical protocol for *in vivo* assessment of the arm vessel deformability.

Methods: A dedicated protocol, applied on 30 volunteers, was specifically designed to estimate both compliance and distensibility of the brachial and radial arteries, and of the basilic and cephalic veins. Bi-dimensional ultrasound imaging was used to acquire cross-sectional areas (CSAs) of arteries in clinostatic configuration, and CSAs of veins combining clinostatic and orthostatic configurations. Arterial pulse pressure was measured with a digital sphygmomanometer, while venous hydrostatic pressure was derived from the arm length in orthostatic configuration.

Results: For each participant, all CSAs were successfully extracted from ultrasound images. The basilic vein and the radial artery exhibited the largest (21.5±8.9 mm^2) and the smallest (3.4±1.0 mm^2) CSAs, respectively; CSA measurements were highly repeatable (Bland-Altman bias <10% and Pearson correlation ≥0.90, for both arteries and veins). In veins, compliance and distensibility were higher than in arteries; compliance was significantly higher (P<0.0001) in the brachial than in the radial artery (3.52×10^{-4} *vs.* 1.3×10^{-4} cm^2/mmHg); it was three times larger in basilic veins than in cephalic veins (17.4×10^{-4} *vs.* 5.6×10^{-4} cm^2/mmHg, P<0.0001).

Conclusions: The proposed non-invasive protocol proved feasible, effective and adequate for daily clinical practice, allowing for the estimation of patient-specific compliance and distensibility of peripheral arteries and veins. If further extended, it may contribute to the fabrication of biohybrid arterio-venous grafts, paving the way towards patient-tailored solutions for vascular access.

Keywords: Peripheral blood vessels; vascular access; ultrasound imaging; compliance; distensibility; hemodialysis

*Please note affiliation 5 is the primary affiliation for this author.

^ ORCID: Alessandro Caimi, 0000-0003-2856-1347; Irene Baroni, 0000-0002-1326-8642; Emiliano Votta, 0000-0001-7115-0151; Stefania A. Riboldi, 0000-0003-4025-6249; Massimiliano M. Marrocco-Trischitta, 0000-0003-1707-9627; Alberto Redaelli, 0000-0002-9020-2188; Francesco Sturla, 0000-0001-7317-304X.

Submitted Oct 08, 2021. Accepted for publication Mar 09, 2022.
doi: 10.21037/qims-21-987
View this article at: https://dx.doi.org/10.21037/qims-21-987

Introduction

Arterio-venous grafts (AVGs) represent a ready-to-use solution to create vascular accesses (VAs) for hemodialysis, especially in patients with failed arterio-venous fistula (AVF), exhausted superficial veins or unsuitable vessels (1). As compared to AVFs, AVGs show lower risk of early failure (i.e., thrombosis or infection) but significantly lower patency 12–18 months after access creation (3–7 years) (2,3). AVGs often undergo occlusion or failure due to the development of intimal hyperplasia close to the venous anastomosis (4). This failure mechanism is generally triggered at the anastomosis by the difference in diameter and compliance between the vessel and the synthetic graft, whose material is significantly stiffer than native tissue (4,5). Accordingly, several studies stressed that adequate tuning of synthetic graft properties is needed to enhance AVG success in VA for hemodialysis: ideally, the graft should be designed to mimic both the diameter and the radial compliance of the native vessel (2,6,7). This is expected to foster more physiological local hemodynamics in the region of the anastomosis, reducing alterations or disturbances of the intraluminal blood shear rate, which plays a major role in the mechanism of graft malfunction and ultimate failure (8,9).

Hence, the quantification of the compliance of peripheral blood vessels is crucial to develop a manufacturing strategy to produce novel compliance-matching devices. If successful, such a strategy could allow for producing multiple and repeatable combinations of graft diameter and compliance, which could be available off-the-shelf for patient-specific tailoring of the graft. However, a gold standard methodology to assess vascular compliance does not exist (10) and *in vivo* estimation still relies on invasive methods requiring intravascular catheterization or the use of pressure transducers, thus inevitably limiting its applicability in daily clinical practice (11,12). Moreover, there is poor consensus regarding the characterization of blood vessels, whose mechanical response can be derived exploiting different parameters such as compliance and distensibility (10,13). Lack of a standardized approach results in wide variability and difficult comparisons among literature data. In addition, vascular mechanics is generally estimated in arterial segments (14-16) and may not be representative of the mechanical behavior over the entire vascular tree, in particular in veins where the use of intravenous catheters is often mandatory (17,18).

Magnetic resonance imaging (MRI) and ultrasound imaging (US) are non-invasive alternatives for the assessment of vascular compliance (10): as compared to the MRI technique, which may be affected by motion artifacts and requires long examinations, US can provide a quicker but reliable assessment of the vessel morphology (19). US imaging is routinely used in patients with end-stage renal disease to monitor the vascular access during hemodialysis (20-22). Though sensitive to the sonographer experience, US technology has been largely employed to estimate arterial vascular compliance (10,23), e.g., for the brachial artery (24). To this purpose, the combined use of US imaging and of a pressure cuff, compressed on the ipsilateral arm, provides input parameters to compute the arterial compliance. However, such a protocol cannot be adopted to investigate the venous compliance, due to the lack of blood pulsatility in the veins.

Herein, we sought to define and test a non-invasive clinical protocol to estimate the radial deformability of the arm vessels. Despite its general potential applicability, the protocol could be of paramount utility for the mechanical characterization of the vessels typically employed for VA creation before hemodialysis. To this purpose, we performed a proof-of-concept analysis on a cohort of healthy subjects to assess both the compliance and the distensibility of the native vessels most commonly used to create bridge-graft configurations, i.e., the brachiocephalic, the brachiobasilic, and the radiocephalic configurations (2,25). The protocol was designed to assess deformability in both the arteries (i.e., brachial and radial) and the veins (i.e., basilic and cephalic) of the arm. Ultrasound imaging was employed to evaluate the cross-sectional area (CSA) of the arteries over the cardiac cycle and of the veins in two specific configurations characterized by different pressure prevalence (26,27).

Hence, the present work aimed to evaluate the feasibility and the reproducibility of the proposed clinical protocol, highlighting its strength and limitations in the assessment of the arm vessels' compliance and distensibility, with potential applicability to the patient-tailored tuning of the mechanical properties of synthetic AVGs for hemodialysis

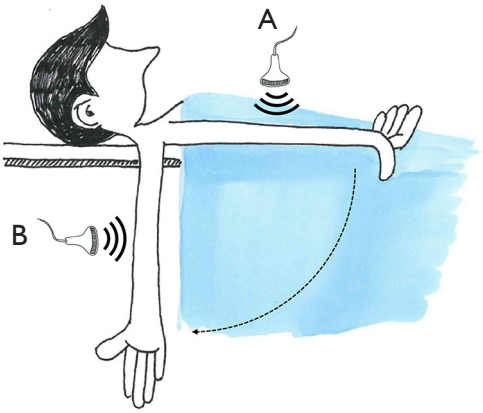

Figure 1 Schematic representation of the (A) clinostatic and (B) orthostatic configurations of the arm used during ultrasound examination. For arteries, only the clinostatic configuration was required; for veins, both arm configurations were exploited.

therapy. We present the following article in accordance with the MDAR checklist (available at https://qims.amegroups.com/article/view/10.21037/qims-21-987/rc).

Methods

Study population

Thirty (n=30) healthy volunteers of Caucasian ethnicity, aged between 20 and 60 years were enrolled in the study. The study was conducted in accordance with the Declaration of Helsinki (as revised in 2013). The local Ethics Committee, i.e., the Ethics Committee of IRCCS Ospedale San Raffaele, approved this study (protocol code "Silkelastograft", No. 32/2020; accepted on February 2nd, 2021). All the subjects provided written informed consent before examination. The analyzed volunteers were subdivided into two sub-groups according to their age, namely "40^-" and "40^+".

Study protocol

A dedicated protocol was designed to quantify the compliance of both arteries and veins of the arm, namely the brachial and radial arteries, the basilic and cephalic veins. The non-invasive protocol employed ultrasound vascular imaging to extract the relevant *in vivo* vessel CSA values, and a digital brachial cuff sphygmomanometer to assess the relevant blood pressure values.

Equipment

Echographic acquisitions were performed on a GE Vivid 7 ultrasound machine (GE Vingmed Ultrasound AS, Horten, Norway), equipped with a bi-dimensional (2D) B-mode transducer vascular linear Array L8-24 probe (Esaote SPA, Genova, Italy). To reduce inter-operator variability, all acquisitions were performed by the same and experienced operator. Systolic (SBP) and diastolic (DBP) pressures were monitored and measured by means of a digital brachial cuff sphygmomanometer (CNAP®, CNSystems Medizintechnik GmbH, Graz, Austria) mounted on the left arm.

Arterial measurements

With the volunteer at rest, lying on the examination table and with both the arms stretched out, i.e., in clinostatic configuration (*Figure 1*), 2D ultrasound imaging was acquired on the right arm over a cardiac cycle. Ultrasound imaging was acquired (I) for the brachial artery, in proximity of the right elbow, next to the vessel distal bifurcation and (II) for the radial artery, in proximity of the right wrist. By analyzing the loop acquisition, the operator identified the systolic and diastolic frames as those characterized by the maximum and minimum cross-sectional dimension, respectively. Contextually, pressures were measured through the digital brachial cuff sphygmomanometer.

Venous measurements

2D imaging was acquired in two specific arm configurations characterized by a different pressure prevalence. First, with the volunteer at rest and in clinostatic position (*Figure 1*), the ultrasound probe was positioned transverse to the arm, above the elbow. Second, the volunteer was asked to stretch the same arm downwards, with the arm outside the examination table but still maintaining the right shoulder on the examination table. This orthostatic configuration induced venous vasodilation due to a column of hydrostatic pressure, whose height was assumed to be comparable to the subject-specific length (l) of the upper-arm, which was measured by means of a ruler as the distance between shoulder and elbow. Since both basilic and cephalic veins are superficial upper-limb veins, the operator paid extreme attention not to compress each vein with the ultrasound probe during the acquisition. Owing to the lack of venous flow pulsatility, static acquisitions were performed.

2D ultrasound image export and post-processing

2D ultrasound images of each selected frame were exported

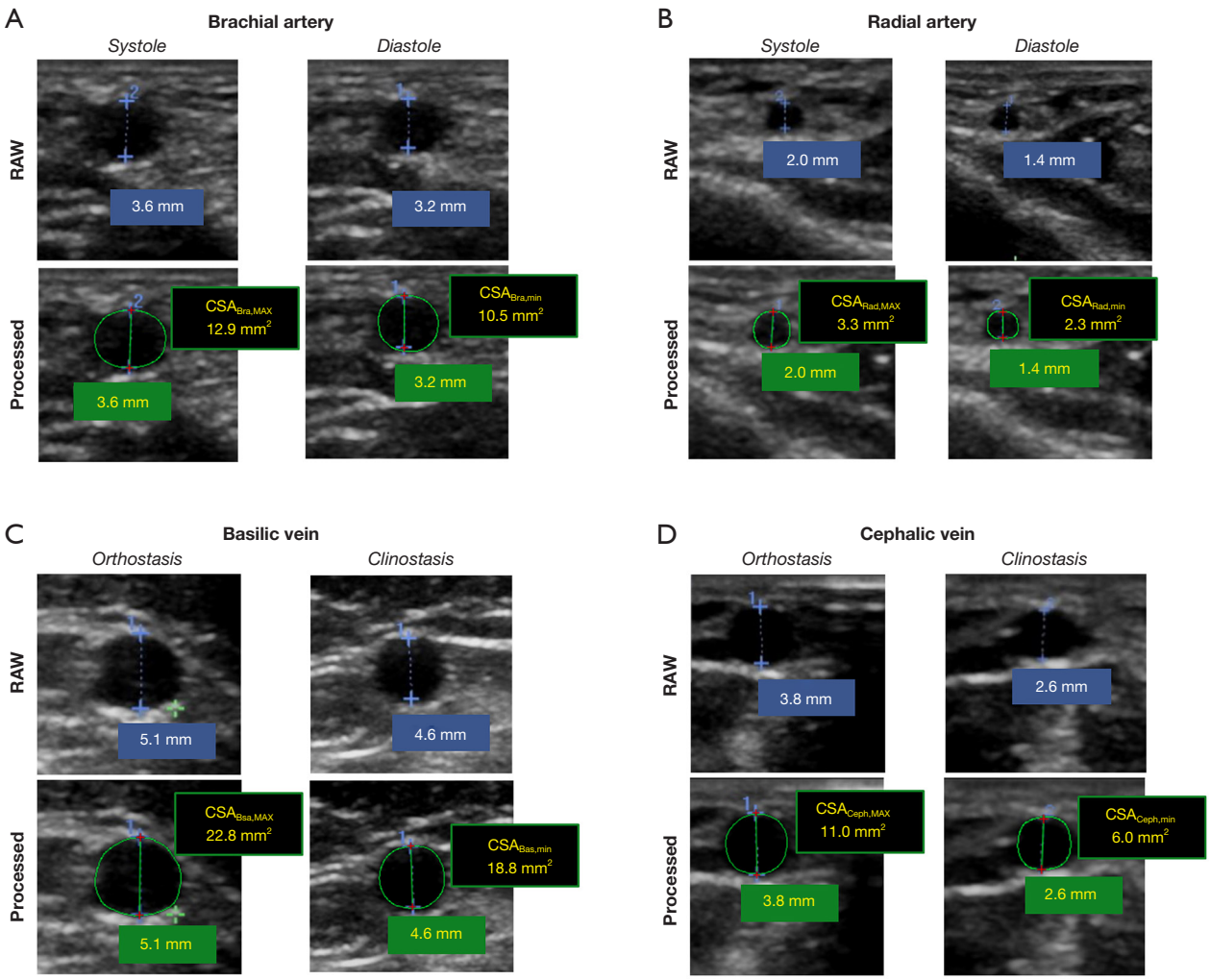

Figure 2 Ultrasound image acquisitions of (A) brachial and (B) radial arteries, and (C) basilic and (D) cephalic veins. For each analysis, a measure of the vessel diameter taken by the operator during ultrasound examination (dotted blue line) was available for offline check; for each vessel, the inner perimeter was segmented (green contour) to derive its cross-sectional area (CSA). Each vessel was analyzed in two different conditions to compute the maximum (MAX) and minimum (min) CSAs: arteries, i.e., brachial (Bra) and radial (Rad), were acquired at systole and diastole while veins, i.e., basilic (Bas) and cephalic (Ceph), under clinostatic and orthostatic conditions.

as DICOM files after the manual measurement of the cross-sectional diameter of each relevant vessel in each relevant frame of the cardiac cycle. These manual measurements were performed to allow for off-line retrieval of information on image pixel spacing in case such information would be not correctly stored in the DICOM file or unreadable by the DICOM viewer. Off-line CSA quantifications were performed in RadiAnt DICOM Viewer 2020.2 (Medixant, Poznan, Poland); the "Closed polygon" tool was employed to delineate the inner perimeter of each vessel (*Figure 2*). The same procedure, repeated for each ultrasound image, yielded the following CSA values for each subject (*Table 1*):

- Maximum ($CSA_{Bra,MAX}$, $CSA_{Rad,MAX}$) and minimum ($CSA_{Bra,min}$, $CSA_{Rad,min}$) CSA of the brachial and radial arteries;
- Maximum ($CSA_{Bas,MAX}$, $CSA_{Ceph,MAX}$) and minimum ($CSA_{Bas,min}$, $CSA_{Ceph,min}$) CSA of the basilic and cephalic veins, obtained from images acquired under orthostatic and clinostatic conditions, respectively.

For each computed CSA, the corresponding equivalent diameter was calculated assuming each section as a circle with equivalent area.

Table 1 Schematic of the analyzed vessel-specific configurations (•) adopted to compute the maximum (MAX) and minimum (min) cross-sectional areas (CSAs) for each vessel; systolic and diastolic configurations were clearly discernable in arteries but not in veins (×)

Vessel	Configuration				CSA	
	Systole	Diastole	Ortho	Clino	MAX	min
Artery						
Brachial (Bra)	•			•	•	
		•		•		•
Radial (Rad)	•			•	•	
		•		•		•
Vein						
Basilic (Bas)	×	×	•		•	
	×	×		•		•
Cephalic (Ceph)	×	×	•		•	
	×	×		•		•

CSA, cross-sectional area; MAX, maximum; min, minimum; Bra, brachial; Rad, radial; Bas, basilic; Ceph, cephalic; Ortho, orthostatic configuration; Clino, clinostatic configuration.

Since off-line CSA required the manual tracing of each vessel contour, we assessed intra-operator and inter-operator variability for both arterial and venous CSAs: for 20 randomly selected datasets, the same operator repeated the tracing twice in different days so to make the second analysis blind to the first one. Also, to assess inter-operator variability two independent operators processed the same datasets in a double-blinded way.

Vessel compliance calculation

For both arteries and veins, compliance (C) was computed as (28):

$$C_x = \frac{CSA_{x,MAX} - CSA_{x,min}}{\Delta P_x} \quad [1]$$

where $x = Bra, Rad, Bas$ and $Ceph$. ΔP was the increase in intraluminal pressure (mmHg) inducing the change in the vessel CSA from $CSA_{x,min}$ to $CSA_{x,MAX}$ and it was computed differently for arteries and veins:

$$\Delta P_x = \begin{cases} (SBP - DBP) & x = Bra, Rad \\ \rho gl & x = Bas, Ceph \end{cases} \quad [2]$$

where (SBP–DBP), used for brachial and radial artery, was the pulse pressure of the patient during the ultrasound acquisition. ρgl, used for veins, was the increase in blood hydrostatic pressure associated with the transition from the clinostatic to the orthostatic vein configuration: blood viscosity ρ was assumed constant and equal to 1,060 Kg/m^3, gravitational acceleration g was equal to 9.81 m/s^2, and l was the length of the analyzed upper-arm, as measured for each volunteer.

Vessel distensibility

Distensibility (D), defined as the relative change in cross-sectional diameter in response to a pressure change (23,29), was expressed as a percentage of the relative diameter change per 100 mmHg, i.e., %/100 *mmHg* (30):

$$D_x = \frac{d_{x,MAX} - d_{x,min}}{d_{x,min} \cdot \Delta P_x} \cdot 10^4 \quad [3]$$

where $d_{x,MAX}$, and $d_{x,MIN}$ were the maximum and minimum equivalent diameters, measured in mm, for each vessel cross-section ($x = Bra$, Rad, Bas and $Ceph$) and ΔP_x was defined as in Eq. [2].

Statistical analysis

Continuous variables were expressed as mean ± standard deviation (SD) or median and interquartile range (25th – 75th percentile) according to the Shapiro-Wilk normality tests; the Chi-square test was adopted to compare categorical variables. Differences in terms of vessel CSA, compliance and distensibility were assessed among the vessels and with respect to age, using non-parametric Friedman analysis and Dunn's multiple comparisons tests. Intra- and inter-observer differences were assessed by means of Bland-Altman plots and Pearson coefficients of correlation (r).

Table 2 Characteristics of participants and blood pressure levels

Characteristics	All (n=30)	40^- (n=15)	40^+ (n=15)	P value[a]
Gender (male/female)	13/17	5/10	8/7	0.46
Age (years)	39±9	31±6	46±6	<0.0001
Height (cm)	170±9	167±11	172±7	0.16
Weight (kg)	64±12	61± 12	68±12	0.14
BSA (m^2)	1.7±0.2	1.7±0.2	1.8±0.2	0.14
BMI (kg/m^2)	22.2±2.5	21.6±2.4	22.7±2.6	0.25
SBP (mmHg)	127 [120–135]	127 [123–131]	125 [114–139]	0.69
DBP (mmHg)	76 [70–83]	75 [70–81]	76 [69–91]	0.66
l (cm)	30±2	29±2	31±2	0.046

Continuous variables expressed as mean ± standard deviation (SD) or median and interquartile range [25^{th}–75^{th} percentile]. [a], unpaired *t* test (Gaussian) or Mann-Whitney test (no Gaussian) between 40^- and 40^+ age subgroups; Chi-square test for categorical variables, i.e., gender. BSA, body surface area (calculated with Du Bois formulation); BMI, body mass index; SBP, systolic blood pressure; DBP, diastolic blood pressure; *l*, upper-arm length; 40^-, sub-group of volunteers with age ≤40 years; 40^+, sub-group of volunteers with age >40 years.

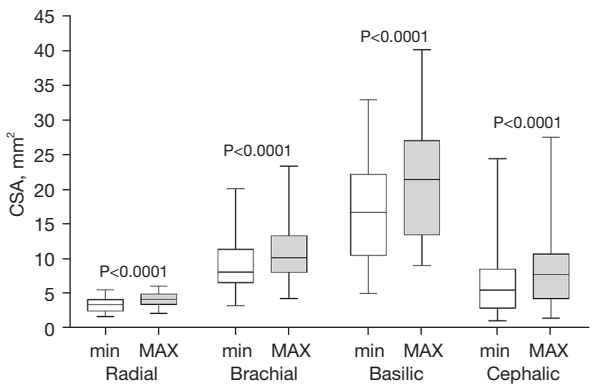

Figure 3 Box (median and interquartile range) and whiskers (minimum and maximum values) plots of the min and MAX CSAs computed for each vessel in the entire study population. Paired *t* test (radial artery and basilic vein) or paired Wilcoxon comparison (brachial artery and cephalic vein) according to the normality of data. min, minimum; MAX, maximum; CSAs, cross-sectional areas.

Statistical analyses were performed using GraphPad Prism 7 (GraphPad Software Inc., La Jolla, CA, USA); a P value <0.05 was considered significant.

Results

Participants characteristics

Subject characteristics and both systolic and diastolic cuff-based pressures are reported in *Table 2* for all the enrolled volunteers. No significant difference between age-based subgroups, i.e., 40^- (n=15) and 40^+ (n=15), was noticed in terms of gender, body surface area (BSA) and body mass index (BMI).

All volunteers exhibited blood pressure levels within the range of normality (31): cohort-averaged arterial SBP and DBP were equal to 127 and 76 mmHg, respectively; no significant differences between 40^- and 40^+ were observed (mean SBP: 127 *vs.* 125 mmHg, P=0.69; mean DBP: 75 *vs.* 76 mmHg, P=0.66).

The mean increase in intraluminal venous pressure from clinostatic to orthostatic vein configuration was equal to 23 mmHg; 40^+ group subjects exhibited a slightly greater increase as compared to 40^- subgroup subjects (24±2 *vs.* 23±2 mmHg, P=0.046), consistently with their statistically longer upper-arm (31±2 *vs.* 29±2 cm, P=0.046).

Vessel cross-sectional area

All CSA values were successfully quantified from ultrasound images for each participant via off-line post-processing (*Figure 3*, Table S1), with no need to exploit the manual measurements performed before exporting the images as DICOM files. The basilic vein exhibited the largest dimensions while the radial artery reported the smallest CSAs. Arterial CSA variations due to systo-diastolic pulse pressure and venous CSA variations due to the transition from clinostatic to orthostatic vessel configuration were all statistically significant (P<0.0001). Percentage mean CSA

Table 3 Bland-Altman results (bias and limits of agreement expressed in mm^2) and Pearson correlation coefficients (*r*) for both inter-observer and intra-observer variability analysis of each vessel CSA

Vessel	CSA	Inter-observer		Intra-observer	
		Bland-Altman	*r*	Bland-Altman	*r*
Radial	Max	−0.4 (−1.3, 0.6)	0.94	−0.1 (−0.9, 0.6)	0.95
	Min	0.1 (−0.6, 0.8)	0.90	−0.4 (−1.1, 0.4)	0.94
Brachial	Max	−0.7 (−2.5, 1.2)	0.98	−0.4 (−1.4, 0.6)	0.99
	Min	0.7 (−1.1, 2.6)	0.97	−0.6 (−1.9, 0.7)	0.99
Basilic	Max	−0.3 (−3.4, 2.8)	0.99	−0.5 (−4.6, 3.6)	0.98
	Min	0.6 (−1.9, 3.3)	0.99	−0.4 (−2.2, 1.3)	0.99
Cephalic	Max	−0.5 (−1.9, 0.9)	0.99	−0.4 (−1.6, 0.8)	0.99
	Min	0.1 (−1.1, 1.1)	0.99	−0.3 (−1.7, 1.1)	0.99

CSA, cross-sectional area; MAX, maximum; Min, minimum.

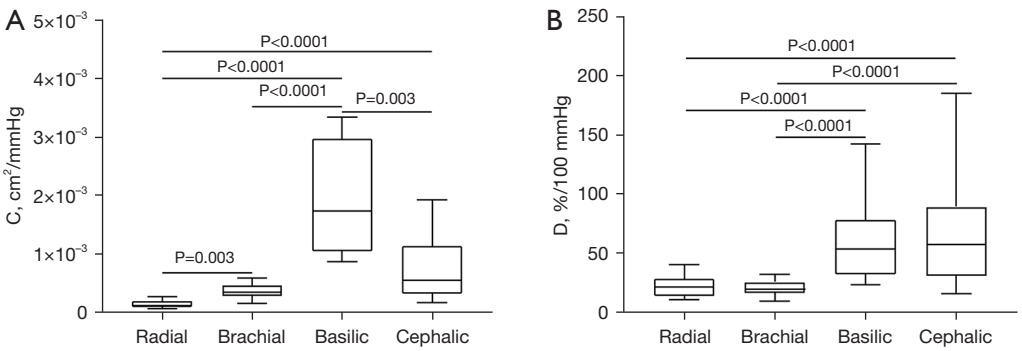

Figure 4 Box (median and interquartile range) and whiskers (10^{th} and 90^{th} percentiles) plots of (A) compliance (C) and (B) distensibility (D) as computed in the whole study population.

increase was highest in veins: from 5.5 to 7.8 mm^2 (+41.8%) and from 16.9 to 21.5 mm^2 (+27.2%) in the cephalic and basilic vein, respectively. CSA increased from 3.4 to 4.2 mm^2 (+23.5%) and from 8.1 to 10.2 mm^2 (+25.9%) in the radial artery and brachial artery, respectively. No statistically significant differences were observed when comparing 40^- and 40^+ subgroups (Table S1).

Intra-observer and inter-observer CSA variability

Bland-Altman analysis (bias and limits of agreement) and Pearson coefficients of correlation (*r*) revealed very good levels of CSA reproducibility between different observers as well as within the same observer (*Table 3*). The entity of Bland-Altman bias was generally below 10% and excellent levels of Pearson correlation were evident for both arteries and veins, with ***r*** ranging between 0.90 and 0.99.

Vessel compliance

The compliance C was greater in veins than in arteries (*Figure 4*). In the brachial artery, C was greater than in the radial artery (3.52×10^{-4} *vs.* 1.3×10^{-4} cm^2/mmHg, P<0.0001, Table S2). C was remarkably greater in the basilic vein than in the cephalic vein (17.4×10^{-4} *vs.* 5.6×10^{-4} cm^2/mmHg, (P<0.0001, Table S2). Differences remained statistically non significant when comparing C between age-based subgroups within the same vessel (*Figure 5*).

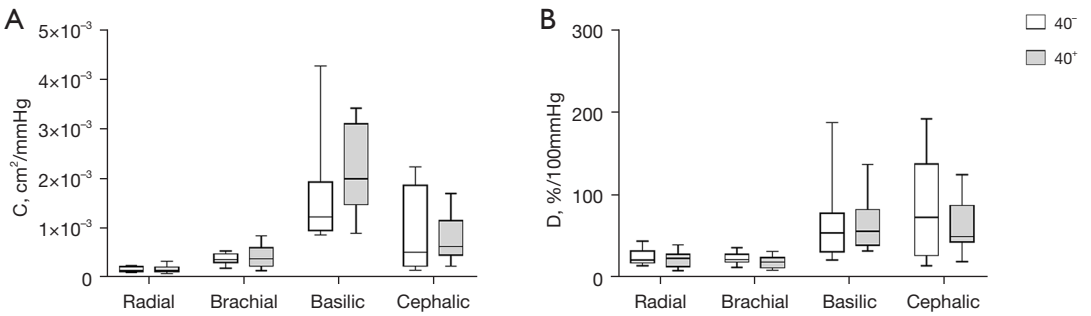

Figure 5 Box (median and interquartile range) and whiskers (10th and 90th percentiles) plots of (A) compliance (C) and (B) distensibility (D) as computed in the two age-based subgroups, i.e., 40^- and 40^+.

Vessel distensibility

Arterial distensibility (*D*) was comparable between the radial and the brachial arteries (median values: 21.5 *vs.* 19.8%/100 mmHg, P>0.99, *Figure 4B*). Venous distensibility was markedly higher than in arteries (P<0.0001): the basilic and the cephalic veins exhibited median *D* values of 54.0%/100 mmHg and 57.5%/100 mmHg, respectively (Table S3). Though the percentage difference between the median values of D_{Ceph} and D_{Bas} was 6.5%, no statistically significant difference was found between the distensibilities of the two veins. Within each vessel, differences were statistically non significant also when comparing *D* between age-based subgroups (*Figure 5B*).

Discussion

In the present study, we proposed a novel and fully non-invasive clinical protocol to estimate the mechanical behavior of both arteries and veins of the arm, combining ultrasound imaging and blood pressure measurements. The protocol, tested on a cohort of 30 healthy volunteers, proved feasible, effective and adequate for daily clinical practice. Indeed, it requires standard echographic equipment and only few minutes, for each subject, to acquire echographic images (two CSAs of the same vessel) in concomitance with arterial blood pressure and a measure of the arm length, thus allowing to estimate both compliance and distensibility of the vessels. Of note, the protocol was designed to be adequate not only for arteries but also for veins through the combination of two different configurations of the arm, i.e., clinostasis and orthostasis, each one associated with a different value of endovenous pressure. Hence, this is a fully non-invasive appraisal to assess *in vivo* venous compliance and distensibility, thus configuring a possible alternative to the use of catheter-based pressure transducers (32).

Both compliance and distensibility were herein computed using an equivalent diameter derived from the vessel CSA, i.e., considering each vessel cross-section as a circle with area equal to its CSA. This strategy differed from previous methods (29,33) employing a direct measure of the diameter, and provided consistent and fully reproducible measurements on veins, which may exhibit an irregular and heterogeneous cross-section shape.

According to our data, the basilic and the cephalic veins reached median levels of distensibility (54.0 and 57.5%/100 mmHg, respectively) significantly higher than the radial (21.5%/100 mmHg) and the brachial arteries (19.8%/100 mmHg). This is an expected result clearly reflecting the inherent differences between arteries and veins in terms of structure and mechanical behavior. Indeed, despite a similar structure, veins are more compliant than arteries due to their thinner wall, in particular for the media layer, and due to a lower amount of elastin (34). It should however be noted that the compliance of a relaxed vein (i.e., at low pressure) is about 10 to 20 times greater than that of an artery while, at high pressure, venous compliance is comparable or smaller than that (35).

Compliance and distensibility quantify the absolute and the relative change, respectively, in the vessel diameter (or area) for a given pressure change (13), and represent complimentary aspects of the vessel behavior. Compliance reflects the buffering function of the vessel (36) and, in the present analysis, pinpointed statistically significant differences between vessels of the same type (*Figure 4A*), i.e., between the radial and the brachial artery (3.52×10^{-4} *vs.* 1.3×10^{-4} cm^2/mmHg, P<0.003) and between the basilic and cephalic veins (17.4×10^{-4} *vs.* 5.6×10^{-4} cm^2/mmHg, P<0.003). Distensibility, by contrast, is related to the

mechanical stiffness of the tissue and physically represents the inverse of the pressure-strain elastic modulus (37) with the pulse pressure and the relative change in diameter corresponding to the vessel wall stress and strain, respectively. In the present analysis, distensibility revealed a significant difference between the cephalic vein and the brachial artery (P<0.0001), which was not detected in terms of compliance (*Figure 4B*). Hence, differences can be appreciated in terms of compliance between vessels sharing a similar function and tissue arrangement while distensibility can further pinpoint the biomechanical comparison between veins and arteries.

Protocol reliability

Though derived from preliminary tests on a small cohort of subjects, the results of our study can be compared against previous data from the scientific literature. Khder and colleagues (38), using ultrasonic echotracking device and simultaneous recording of continuous pressure by digital photoplethysmography, estimated the compliance of the right radial artery about 5 cm proximal to the wrist in a cohort of normal subjects (n=41) and obtained a mean value of cross-sectional compliance equal to 3.61×10^{-5} cm^2/mmHg. The mean value of radial artery compliance obtained in our cohort, i.e., C=1.3×10^{-4} cm^2/mmHg, markedly exceeds the one by Khder *et al.* and this could be due to differences between the two considered populations. Indeed, our subjects were generally younger (mean age of 39 *vs.* 52 years), reported lower values of arterial pulse pressure (50 *vs.* 59 mmHg) and a higher systole-to-diastole CSA increase ascribable to a smaller diameter at diastole (2.1 *vs.* 2.8 mm), this probably being associated with the higher percentage of female subjects in our cohort study, i.e., 57% *vs.* 39%.

In a small cohort of normocholesteromic subjects (mean age 45 years, SBP and DBP equal to 115 and 69 mmHg, respectively), Giannattasio *et al.* reported a mean value of radial artery compliance of about 5.1×10^{-5} cm^2/mmHg using echotracking combined with photopletysmographic recording of blood pressure (14).

In our analysis, the measure of radial artery diameter was equal to 2.2±0.3 mm and well compared with the ultrasound measure, equal to 2.2±0.4 mm, performed by Velasco *et al.* on a population of healthy volunteers (n=100) with an average age of 35 years (39).

As far as the analysis of veins is concerned, changes in venous CSA were reliably measured in response to a change in posture, with pressure derived from the corresponding variation of hydrostatic pressure (27). For instance, the cephalic vein reported clinostastic and orthostatic CSA medians equal to 5.5 and 7.8 mm^2, respectively, and these changes were associated with a mean variation of hydrostatic pressure equal to 23 mmHg. These measures well agree with the mean value of cephalic CSA, i.e., about 8 mm^2, reported by Planken *et al.* at a venous congestion pressure of 20 mmHg in a cohort of 10 healthy subjects (mean age of 26 years) using transverse B-mode ultrasonography (40).

Of note, veins reported a data variance higher than arteries: this may be primarily due to the more heterogeneous shape and dimension of veins, which are also more superficial than arteries and, thus, more sensitive to external solicitations. In addition, the ultrasound imaging protocol for veins (based on two different arm configurations) as well as the venous pulse pressure estimation based on the upper-arm length (not statistically comparable between the enrolled subjects, i.e., P=0.046) may have contributed to the increased dispersion of venous data.

Though intravascular catheterization can provide accurate measurements, data are lacking in the literature to specifically compare, for the same peripheral vessels herein analyzed, our non-invasive measurements against invasive catheter-based methods. Indeed, patients undergoing hemodialysis are routinely examined through non-invasive ultrasound imaging (21) and the use of invasive monitoring could result detrimental in these patients, whose limbs are severely plagued by multiple, repeated and painful accesses necessary for the therapeutic treatment.

Clinical perspective

The feasibility of the proposed protocol makes it suitable for the non-invasive estimation of the mechanical properties of peripheral vessels.

In this perspective, the protocol capability to systematically characterize and differentiate the mechanical response of specific arterial and venous vessels will have a direct impact on the improvement of AVGs manufacturing, in that it could pave the way to the development of a new generation of grafts, whose mechanical properties could be optimized for specific categories of recipients. Expanding the proposed analysis to real patients requiring AVGs (e.g., patients undergoing hemodialysis), *in vivo* data of compliance and distensibility will improve the current knowledge of the mechanical behavior of native arteries and veins. Exactly as it happens with geometrical graft dimensions, AVGs could be produced and catalogued off-

the-shelf according to the different ranges of mechanical properties. Hence, a systematic and standardized characterization of the vessel mechanical properties, through *in vivo* non-invasive measurements on real patients requiring AVGs, will support surgeon in the selection of the most adequate graft according to the specific clinical target.

Furthermore, capitalizing on the continuously evolving manufacturing technologies such as electrospinning and on the tuning of promising hybrid materials as the fibroin/polyurethane combinations (41-43), *in vivo* ground-truth data will be crucial to further personalize the technology of hybrid vascular grafts according to the patient-specific *in vivo* characteristics.

The applicability of the present protocol could be easily extended to other clinically relevant scenarios. For instance, in case of coronary artery bypass graft (CABG) surgery, a healthy blood vessel from the leg (e.g., the saphenous vein) or the chest (e.g., the mammary artery) is explanted from its native site and used as heterotopic and autologous graft to bypass the blocked coronary artery and restore blood flow and oxygen supply to myocardium (35). To guide the selection of graft for CABG on a patient-specific basis, the compliance of peripheral vessels could be assessed and compared, thus providing additional insight into the mechanical behavior of the available autologous substitutes for CABG.

Limitations

The following limitations should be taken into account when interpreting the results of the study.

First, we herein analyzed a small cohort of healthy volunteers only. Accordingly, the current analysis provided preliminary results, which should be further extended and confirmed on a larger population, also including real patients, e.g., patients requiring vascular access via AVG to undergo hemodialysis. Nonetheless, in the present proof-of-concept analysis, we successfully tested the validity of the proposed protocol and its technical feasibility in clinical practice. Furthermore, gender-based differences were not explored due to a non-homogeneous partition between male and female subjects enrolled in the study.

Second, all the enrolled subjects were designedly aged between 20 and 60 years old and this did not allow to effectively investigate the influence of aging, which is generally associated with vessel wall remodeling and stiffening (44,45). To deepen age-related differences, the study population should be further extended including elderly people, i.e., largely over 60 years old (45).

Third, the lumen of each vessel was processed through a manual segmentation procedure and the arterial CSAs were extracted from a single cardiac cycle only. Though a manual imaging processing was considered adequate for the purpose of the present proof of concept analysis, further efforts will be required to automatize image processing, e.g., exploiting speckle-tracking methods to automatically track and assess the vessel CSA over multiple cardiac cycles (37,46,47). This will allow to definitively extend the analysis to larger populations.

Fourth, the protocol is sensitive to the anatomic variability of subjects and the accuracy of CSA delineation is influenced by the dimension of the vessel itself, in particular when small vessels, e.g., the radial artery, are considered. Though the protocol proved to be effective also in case of CSA measurements for small peripheral vessels, future automation of the ultrasound imaging processing will allow to further reduce observer variability and enhance data reproducibility.

Conclusions

We herein proposed a user-friendly novel clinical protocol to evaluate the mechanical properties of peripheral arteries and veins, focusing in particular on the ones commonly used for vascular access in hemodialysis. If further extended and validated, the present protocol may pave the way towards patient-tailored solutions for vascular access.

Acknowledgments

We want to thank Prof. Simone Vesentini for the creation of the illustration reported in *Figure 1*.
Funding: This work was part of the SILKELASTOGRAFT project, partially funded by Fondazione Cariplo and Regione Lombardia within the framework of the grant "Avviso congiunto per la concessione di contributi a sostegno del trasferimento della conoscenza nel settore dei Materiali avanzati" (No. 2018-1777). This work was supported by IRCCS Policlinico San Donato, a clinical research hospital partially funded by the Italian Ministry of Health.

Footnote

Reporting Checklist: The authors have completed the MDAR checklist. Available at https://qims.amegroups.com/article/

view/10.21037/qims-21-987/rc

Conflicts of Interest: All authors have completed the ICMJE uniform disclosure form (available at https://qims.amegroups.com/article/view/10.21037/qims-21-987/coif). AC is employed at Bioengineering Laboratories Srl, which is partner of the SILKELASTOGRAFT project and major shareholder of Dialybrid Srl. SC and SAR are employed at Dialybrid Srl; SAR is co-inventor of patents concerning vascular grafts. The other authors have no conflicts of interest to declare.

Ethical Statement: The authors are accountable for all aspects of the work by ensuring that questions related to the accuracy or integrity of any part of the work are appropriately investigated and resolved. The study was conducted in accordance with the Declaration of Helsinki (as revised in 2013). The local Ethics Committee, i.e., Ethics Committee of IRCCS Ospedale San Raffaele, approved this study (protocol code "Silkelastograft", No. 32/2020; accepted on February 2nd, 2021). All the subjects provided written informed consent before examination.

References

1. Akoh JA. Prosthetic arteriovenous grafts for hemodialysis. J Vasc Access 2009;10:137-47.
2. Bittl JA. Catheter Interventions for Hemodialysis Fistulas and Grafts. JACC Cardiovasc Interv 2010;3:1-11.
3. Voorzaat BM, Janmaat CJ, van der Bogt KEA, Dekker FW, Rotmans JI. Patency Outcomes of Arteriovenous Fistulas and Grafts for Hemodialysis Access: A Trade-Off between Nonmaturation and Long-Term Complications. Kidney360 2020;1:916-24.
4. Salacinski HJ, Goldner S, Giudiceandrea A, Hamilton G, Seifalian AM, Edwards A, Carson RJ. The mechanical behavior of vascular grafts: a review. J Biomater Appl 2001;15:241-78.
5. Remuzzi A, Ene-Iordache B. Novel paradigms for dialysis vascular access: upstream hemodynamics and vascular remodeling in dialysis access stenosis. Clin J Am Soc Nephrol 2013;8:2186-93.
6. Abbott WM, Megerman J, Hasson JE, L'Italien G, Warnock DF. Effect of compliance mismatch on vascular graft patency. J Vasc Surg 1987;5:376-82.
7. Peck MK, Dusserre N, Zagalski K, Garrido SA, Wystrychowski W, Glickman MH, Chronos NA, Cierpka L, L'Heureux N, McAllister TN. New biological solutions for hemodialysis access. J Vasc Access 2011;12:185-92.
8. Leuprecht A, Perktold K, Prosi M, Berk T, Trubel W, Schima H. Numerical study of hemodynamics and wall mechanics in distal end-to-side anastomoses of bypass grafts. J Biomech 2002;35:225-36.
9. Post A, Diaz-Rodriguez P, Balouch B, Paulsen S, Wu S, Miller J, et al. Elucidating the role of graft compliance mismatch on intimal hyperplasia using an ex vivo organ culture model. Acta Biomater 2019;89:84-94.
10. Glasser SP, Arnett DK, McVeigh GE, Finkelstein SM, Bank AJ, Morgan DJ, Cohn JN. Vascular compliance and cardiovascular disease: a risk factor or a marker? Am J Hypertens 1997;10:1175-89.
11. Cohn JN. Arterial compliance to stratify cardiovascular risk: more precision in therapeutic decision making. Am J Hypertens 2001;14:258S-63S.
12. Sharath U, Shwetha C, Anand K, Asokan S. Radial arterial compliance measurement by fiber Bragg grating pulse recorder. J Hum Hypertens 2014;28:736-42.
13. Parati G, Bernardi L. How to assess arterial compliance in humans. J Hypertens 2006;24:1009-12.
14. Giannattasio C, Mangoni AA, Failla M, Carugo S, Stella ML, Stefanoni P, Grassi G, Vergani C, Mancia G. Impaired radial artery compliance in normotensive subjects with familial hypercholesterolemia. Atherosclerosis 1996;124:249-60.
15. Manini S, Passera K, Huberts W, Botti L, Antiga L, Remuzzi A. Computational model for simulation of vascular adaptation following vascular access surgery in haemodialysis patients. Comput Methods Biomech Biomed Engin 2014;17:1358-67.
16. Covic A, Gusbeth-Tatomir P, Goldsmith DJ. Arterial stiffness in renal patients: an update. Am J Kidney Dis 2005;45:965-77.
17. Sperry BW, Campbell J, Yanavitski M, Kapadia S, Tang WHW, Hanna M. Peripheral Venous Pressure Measurements in Patients With Acute Decompensated Heart Failure (PVP-HF). Circ Heart Fail

2017;10:e004130.
18. Sanfilippo F, Noto A, Martucci G, Farbo M, Burgio G, Biasucci DG. Central venous pressure monitoring via peripherally or centrally inserted central catheters: a systematic review and meta-analysis. J Vasc Access 2017;18:273-8.
19. Reimer P, Landwehr P. Non-invasive vascular imaging of peripheral vessels. Eur Radiol 1998;8:858-72.
20. Lomonte C, Meola M, Petrucci I, Casucci F, Basile C. The key role of color Doppler ultrasound in the work-up of hemodialysis vascular access. Semin Dial 2015;28:211-5.
21. Nalesso F, Garzotto F, Petrucci I, Samoni S, Virzì GM, Gregori D, Meola M, Ronco C. Standardized Protocol for Hemodialysis Vascular Access Assessment: The Role of Ultrasound and ColorDoppler. Blood Purif 2018;45:260-9.
22. Lok CE, Huber TS, Lee T, Shenoy S, Yevzlin AS, Abreo K, et al. KDOQI Clinical Practice Guideline for Vascular Access: 2019 Update. Am J Kidney Dis 2020;75:S1-164.
23. Mackenzie IS, Wilkinson IB, Cockcroft JR. Assessment of arterial stiffness in clinical practice. QJM 2002;95:67-74.
24. Weitzel WF, Kim K, Rubin JM, Xie H, O'Donnell M. Renal Advances in Ultrasound Elasticity Imaging: Measuring the Compliance of Arteries and Kidneys in End-Stage Renal Disease. Blood Purif 2005;23:10-7.
25. Melnick DM. Vascular access for hemodialysis. Illustrative Handbook of General Surgery: Second Edition. 2016. 747-757 p.
26. Zamboni P, Tavoni V, Sisini F, Pedriali M, Rimondi E, Tessari M, et al. Venous compliance and clinical implications. Veins Lymphat 2018;7:49-55.
27. Tansey EA, Montgomery LEA, Quinn JG, Roe SM, Johnson CD. Understanding basic vein physiology and venous blood pressure through simple physical assessments. Adv Physiol Educ 2019;43:423-9.
28. Cavalcante JL, Lima JAC, Redheuil A, Al-Mallah MH. Aortic stiffness: Current understanding and future directions. J Am Coll Cardiol 2011;57:1511-22.
29. Segers P, Rietzschel ER, Chirinos JA. How to Measure Arterial Stiffness in Humans. Arterioscler Thromb Vasc Biol 2020;40:1034-43.
30. International Standard ISO 7198:2016 Cardiovascular implants and extracorporeal systems — Vascular prostheses — Tubular vascular grafts and vascular patches. Available online: www.iso.org/standard/50661.html
31. Mancia G, De Backer G, Dominiczak A, Cifkova R, Fagard R, Germano G, et al. 2007 Guidelines for the Management of Arterial Hypertension: The Task Force for the Management of Arterial Hypertension of the European Society of Hypertension (ESH) and of the European Society of Cardiology (ESC). J Hypertens 2007;25:1105-87.
32. Zamboni P, Marcellino MG, Portaluppi F, Manfredini R, Feo C V, Quaglio D, et al. The relationship between in vitro and in vivo venous compliance measurement. Int Angiol 1996;15:149-52.
33. Gamble G, Zorn J, Sanders G, MacMahon S, Sharpe N. Estimation of arterial stiffness, compliance, and distensibility from M-mode ultrasound measurements of the common carotid artery. Stroke 1994;25:11-6.
34. Camasão DB, Mantovani D. The mechanical characterization of blood vessels and their substitutes in the continuous quest for physiological-relevant performances. A critical review. Mater Today Bio 2021;10:100106.
35. Ghista DN, Kabinejadian F. Coronary artery bypass grafting hemodynamics and anastomosis design: a biomedical engineering review. Biomed Eng Online 2013;12:129.
36. Van Bortel LM, Kool MJ, Boudier HA, Struijker Boudier HA. Effects of antihypertensive agents on local arterial distensibility and compliance. Hypertension 1995;26:531-4.
37. Zheng Y, Thelen BJ, Rajaram N, Krishnamurthy VN, Hamilton J, Funes-Lora MA, Morgan T, Yessayan L, Bishop B, Osborne N, Henke P, Shih AJ, Weitzel WF. Angioplasty Induced Changes in Dialysis Vascular Access Compliance. Ann Biomed Eng 2021;49:2635-45.
38. Khder Y, Bray-Desboscs L, Aliot E, Zannad F. Effects of blood pressure control on radial artery diameter and compliance in hypertensive patients. Am J Hypertens 1997;10:269-74.
39. Velasco A, Ono C, Nugent K, Tarwater P, Kumar A. Ultrasonic evaluation of the radial artery diameter in a local population from Texas. J Invasive Cardiol 2012;24:339-41.
40. Planken RN, Keuter XH, Kessels AG, Hoeks AP, Leiner T, Tordoir JH. Forearm cephalic vein cross-sectional area changes at incremental congestion pressures: towards a standardized and reproducible vein mapping protocol. J Vasc Surg 2006;44:353-8.
41. van Uden S, Catto V, Perotto G, Athanassiou A, Redaelli ACL, Greco FG, Riboldi SA. Electrospun fibroin/polyurethane hybrid meshes: Manufacturing, characterization, and potentialities as substrates for haemodialysis arteriovenous grafts. J Biomed Mater Res B Appl Biomater 2019;107:807-17.
42. van Uden S, Vanerio N, Catto V, Bonandrini B, Tironi M,

Figliuzzi M, et al. A novel hybrid silk-fibroin/polyurethane three-layered vascular graft: Towards in situ tissue-engineered vascular accesses for haemodialysis. Biomed Mater 2019;14:025007.
43. Riboldi SA, Tozzi M, Bagardi M, Ravasio G, Cigalino G, Crippa L, Piccolo S, Nahal A, Spandri M, Catto V, Tironi M, Greco FG, Remuzzi A, Acocella F. A Novel Hybrid Silk Fibroin/Polyurethane Arteriovenous Graft for Hemodialysis: Proof-of-Concept Animal Study in an Ovine Model. Adv Healthc Mater 2020;9:e2000794.
44. Kohn JC, Lampi MC, Reinhart-King CA. Age-related vascular stiffening: causes and consequences. Front Genet 2015;6:112.
45. Lopes A, Lloret-Linares C, Simoneau G, Levy B, Bergmann JF, Mouly S. Impact of physiological aging on lower limb venous compliance. Eur Geriatr Med 2013;4:133-8.
46. Weitzel WF, Rajaram N, Zheng Y, Thelen BJ, Krishnamurthy VN, Hamilton J, et al. Ultrasound speckle tracking to detect vascular distensibility changes from angioplasty and branch ligation in a radio-cephalic fistula: Use of novel open source software. J Vasc Access 2020. [Epub ahead of print].
47. Funes-Lora MA, Thelen BJ, Shih AJ, Hamilton J, Rajaram N, Lyu J, Zheng Y, Morgan T, Weitzel WF. Ultrasound Measurement of Vascular Distensibility Based on Edge Detection and Speckle Tracking Using Ultrasound DICOM Data. ASAIO J 2022;68:112-21.

Cite this article as: Cappelletti S, Caimi A, Caldiroli A, Baroni I, Votta E, Riboldi SA, Marrocco-Trischitta MM, Redaelli A, Sturla F. Non-invasive estimation of vascular compliance and distensibility in the arm vessels: a novel ultrasound-based protocol. Quant Imaging Med Surg 2022;12(7):3515-3527. doi: 10.21037/qims-21-987

Supplementary

Table S1 Maxima and minima cross-sectional areas (CSA) of each vessel considering the whole population (All), and the two age sub-groups (40^-, 40^+). Values are expressed in mm^2

	CSA	All (n=30)	40^- (n=15)	40^+ (n=15)	P-value[a]
Radial artery	Max	4.2 ± 1.0	3.9 ± 1.1	4.5 ± 0.9	0.12
	Min	3.4 ± 1.0	3.1 ± 1.0	3.8 ± 0.8	0.07
Brachial artery	Max	10.2 (8.1–13.3)	9.0 (6.8–12.9)	10.9 (8.3–14.9)	0.20
	Min	8.1 (6.6–11.4)	7.1 (5.1–10.7)	8.3 (7.4–12.2)	0.15
Basilic vein	Max	21.5 ± 8.9	20.3 ± 8.3	22.9 ± 9.6	0.45
	Min	16.9 ± 8.2	16.6 ± 8.1	17.6 ± 8.5	0.64
Cephalic vein	Max	7.8 (4.3–10.7)	8.5 (3.9–10.4)	7.1 (4.4–14.2)	0.23
	Min	5.5 (2.9–8.5)	6.0 (2.8–8.4)	5.3 (3.5–11.7)	0.20

Continuous variables expressed as mean ± standard deviation or median and interquartile range (IQR); [a]Comparison (*t* test) between 40^- and 40^+ age sub-groups.

Table S2 Compliance (*C*) of vessels in the whole population (All), and in the two age subgroups (40^- and 40^+); values expressed as 10^{-4} cm^2/mmHg

	All (n=30)	40^- (n=15)	40^+ (n=15)	P-value[a]
Radial artery	1.3 (1.0–2.1)	1.2 (1.0–2.1)	1.3 (1.0–2.0)	0.67
Brachial artery	3.52 (2.9–4.7)	3.5 (2.9–4.6)	3.7 (2.2–6.0)	0.49
Basilic vein	17.4 (10.6–29.7)	12.1 (9.4–19.2)	20.0 (14.6–31.0)	0.42
Cephalic vein	5.6 (3.3–11.5)	5.0 (2.2–18.5)	6.2 (4.4–11.4)	0.88

Continuous variables expressed as mean ± standard deviation or median and interquartile range (IQR); [a]Comparison (*t* test) between 40^- and 40^+ age sub-groups.

Table S3 Distensibility (*D*) of vessels in the whole population (All), and in the two age subgroups (40^- and 40^+); values expressed as %/100mmHg

	All (n=30)	40^- (n=15)	40^+ (n=15)	P-value[a]
Radial artery	21.5 (14.2–28.5)	20.5 (16.9–31.3)	22.5 (12.7–27.6)	0.47
Brachial artery	19.8 (16.4–28.8)	21.0 (18.2–27.3)	18.1 (11.1–23.3)	0.16
Basilic vein	54.0 (32.4–78.5)	53.4 (30.4–77.4)	55.1 (38.4–81.6)	0.99
Cephalic vein	57.5 (31.0–89.4)	72.3 (25.9–137.4)	48.8 (42.7–86.6)	0.33

Continuous variables expressed as mean ± standard deviation or median and interquartile range (IQR); [a]Comparison (*t* test) between 40^- and 40^+ age sub-groups.

https://dx.doi.org/10.21037/qims-21-987